

## A rapid competitive ELISA assay of Okadaic acid level based on epoxy-functionalized magnetic beads

Linjiang Pang, Haoran Quan, Ying Sun, Pingya Wang, Daifu Ma, Pengqian Mu, Tingting Chai, Yiming Zhang & Bruce D. Hammock

To cite this article: Linjiang Pang, Haoran Quan, Ying Sun, Pingya Wang, Daifu Ma, Pengqian Mu, Tingting Chai, Yiming Zhang & Bruce D. Hammock (2019) A rapid competitive ELISA assay of Okadaic acid level based on epoxy-functionalized magnetic beads, Food and Agricultural Immunology, 30:1, 1286-1302, DOI: [10.1080/09540105.2019.1689231](https://doi.org/10.1080/09540105.2019.1689231)

To link to this article: <https://doi.org/10.1080/09540105.2019.1689231>



© 2019 Zhejiang A&F University. Published by Informa UK Limited, trading as Taylor & Francis Group



[View supplementary material](#)



Published online: 14 Nov 2019.



[Submit your article to this journal](#)



Article views: 593



[View related articles](#)



[View Crossmark data](#)



Citing articles: 4 [View citing articles](#)

## A rapid competitive ELISA assay of Okadaic acid level based on epoxy-functionalized magnetic beads

Linjiang Pang<sup>a</sup>, Haoran Quan<sup>a</sup>, Ying Sun<sup>b</sup>, Pingya Wang<sup>b</sup>, Daifu Ma<sup>c</sup>, Pengqian Mu<sup>d</sup>, Tingting Chai<sup>a</sup>, Yiming Zhang <sup>a</sup> and Bruce D. Hammock<sup>e</sup>

<sup>a</sup>School of Agriculture and Food Science, Zhejiang A&F University, Hangzhou, People's Republic of China; <sup>b</sup>Institute of Food and Drug Inspection and Testing Research of Zhoushan, Zhoushan, People's Republic of China; <sup>c</sup>Xuzhou Institute of Agricultural Sciences of the Xuhuai District of Jiangsu Province, Xuzhou, People's Republic of China; <sup>d</sup>China Asia Pacific Application Support Center, AB SCIEX, Shanghai, People's Republic of China; <sup>e</sup>Department of Entomology and UCD Comprehensive Cancer Center, University of California, Davis, CA, USA

### ABSTRACT

Using newly designed epoxy group activated carbon shell magnetic beads as a goat against mouse antibody (G-Mab) carrier, a competitive immunoassay was conducted on the surface of G-Mab-coated magnetic beads (G-Mab-MBs). Mouse monoclonal antibody against Okadaic acid (Mab), Okadaic acid-horseradish peroxidase conjugate (OA-HRP) and OA were simultaneously added into a reaction system. The enzyme-linked immunosorbent assay (ELISA) was performed in a 96-well microplate incorporated with magnetic bars. Detection of the OA level by using the current approach provided an excellent linear relationship in the range of 0.35–25.0  $\mu\text{g L}^{-1}$  with a half-maximal inhibitory concentration  $\text{IC}_{50}$  of 3.27  $\mu\text{g L}^{-1}$  and LOD values of 0.35  $\mu\text{g L}^{-1}$ . The shellfish matrix and other algal toxins presented in the sample extraction did not produce obvious interference. As a comparison, tests were conducted via commercial ELISA and liquid chromatography-tandem mass spectrometry (LC-MS/MS), and the corresponding analytical results demonstrated the reliability of the current protocol.

**Abbreviations:** OA: Okadaic acid; DSP: diarrhetic Shellfish Poisoning; DTX-1: dinophysistoxin-1; PSP: paralytic shellfish poisoning; TTX: tetrodotoxin-Tetrodotoxin; MC: microcystins; NSP: neurotoxic shellfish toxin; ASP: amnesic shellfish toxin; GTX-2,3: gynotoxin2&3; TMB: 3,3',5,5'-Tetramethylbenzidine; HRP: horseradish Peroxidase; G-Mab: goat against mouse antibody; G-Mab-MBs: goat against mouse antibody coated magnetic beads; MAb: mouse monoclonal antibody against Okadaic acid; DMSO: dimethylsulfoxide; PBS: phosphate buffered saline; BSA: bovine serum albumin; polyethylene glycol (PEG 10000); CBS: carbonate buffer; PBST (1 $\times$ , pH = 7.4, containing 0.05% Tween-20); IR (inhibitory rate, %)

### ARTICLE HISTORY

Received 2 October 2019  
Accepted 31 October 2019

### KEYWORDS

Magnetic beads; epoxy-functionalized; Okadaic acid; ELISA; seafood sample

**CONTACT** Yiming Zhang  [zym7307@zju.edu.cn](mailto:zym7307@zju.edu.cn)  School of Agriculture and Food Science, Zhejiang A&F University, Hangzhou, 311300, People's Republic of China

 Supplemental data for this article can be accessed at <https://doi.org/10.1080/09540105.2019.1689231>.

© 2019 Zhejiang A&F University. Published by Informa UK Limited, trading as Taylor & Francis Group  
This is an Open Access article distributed under the terms of the Creative Commons Attribution-NonCommercial-NoDerivatives License (<http://creativecommons.org/licenses/by-nc-nd/4.0/>), which permits non-commercial re-use, distribution, and reproduction in any medium, provided the original work is properly cited, and is not altered, transformed, or built upon in any way.

## 1. Introduction

Okadaic acid (OA) is a typical component of diarrhetic shellfish poisoning (DSP) and is widely distributed in sea areas. Intake of OA might produce a series of acute or chronic health risks such as gastrointestinal disorders including diarrhea, abdominal pain, nausea, and vomiting (Paredes, Rietjens, Vieites, & Cabado, 2011; Suganuma et al., 1988). Due to its health risk, the European Food Safety Authority (EFSA) suggested that a maximum permitted level of OA in shellfish tissues should be reduced from 160 to 45  $\mu\text{g kg}^{-1}$ . Recently, a report indicated that some commercially available seafood from the coastal cities in China may be inedible due to serious marine toxin contamination (Lin et al., 2015). Therefore, precise detection of OA residue in shellfish or mussel products is critical for monitoring aquatic product safety.

A series of bioassay methods or instrumental analytical strategies have been applied to the determination of the OA concentration in seafood products, such as mouse bioassay (Prassopoulou, Katikou, Georgantelis, & Kyritsakis, 2009), ELISA kit (Liu, Hung, Lu, Chou, & Yu, 2014; Lu et al., 2012), and high-performance liquid chromatography (HPLC) and/or tandem mass spectrometer techniques (Stengel & Connan, 2015; Wu, Wang, Sun, & Liu, 2015; Zendong et al., 2015). In addition, chemiluminescence immunoassay technology offered an alternative high sensitive analysis of the OA concentration with a detection limit of 0.0098  $\mu\text{g kg}^{-1}$  (Lin et al., 2014). Compared with confirmatory instrumental approaches, biosensor and nanotechnology for diagnostics could provide rapid screening results and the availability of specific and on-site detection (Hayat, Barthelmebs, Sassolas, & Marty, 2012; Llamas et al., 2007; Su, Qiu, Fang, Zou, & Wang, 2017; Yakes, Buijs, Elliott, & Campbell, 2016). For example, versatile designed lateral-flow immunoassay (LFIA) technology based on colloidal gold or Fluorescent microspheres provides alternative rapid protocols (Jawaid et al., 2015; Lu et al., 2012).

As traditional analytical protocols, ELISA methods are widely considered to be valid and effective methods for food or drug safety determination (Garthwaite et al., 2001; Pleadin et al., 2014). Because of their easy-operation and good reproducibility, ELISA approaches have been conveniently applied in food analytical labs worldwide for screening purposes, and the data obtained can be used for a meta-analysis source with confidence (Kolossova, Shim, Yang, Eremin, & Chung, 2006). Currently, many types of commercial ELISA kits based on different approaches, such as sandwich or competitive immunoassay, can be provided by biological companies. However, with regard to trace contaminants and natural toxin analysis, the analytical performance of ELISA was deserved to be improved, and the development and production of novel antibodies have been reported to be an effective strategy (Li et al., 2018; Liu et al., 2014). Moreover, through combination with the introduction of biocompatible nanomaterial into biological assays, traditional ELISA technologies have made great progress in recent years (Radoi, Targa, Prieto-simon, & Marty, 2008; Wang, Niessner, Tang, & Knopp, 2016). In particular, the possible miniaturization and the incorporation of nanomaterials are bringing a portability of “point-of-use” and availability of rapid screening analysis based on traditional platforms. Therefore, it is of great significance to continuously develop and innovate rapid detection methods based on the ELISA approach.

Magnetic beads (MBs) have been widely exploited as carriers in bioassay and immunoassay (Agrawal, Sathe, & Nie, 2007; Dominguez et al., 2012; Eissa et al., 2013; Jamshaid et al., 2016; Schneck, Phinney, Lee, & Lowenthal, 2016; Tetala & Vijayalakshmi, 2016). Because of the inherent advantages such as ease of isolation, diversified surface functionalization and good biocompatibility, MBs can be used for clean-up and isolation, and serve as a bioinspired supporting carrier or even a sensing platform in the field of food rapid analysis. Hayat and coworkers proposed a label-free amperometric immunosensor based on the protein G-coated magnetic beads, which were endowed gold electrodes with highly sensitive immunoassay active sites. The limit of detection (LOD) ( $0.5 \mu\text{g L}^{-1}$ ) obtained was lower than that ( $1.0 \mu\text{g L}^{-1}$ ) of a simultaneous colorimetric immunoassay, which was based on a direct competitive strategy (Hayat et al., 2012). Dominguez developed an indirect competitive immunoassay method with an LOD of  $0.15 \mu\text{g L}^{-1}$  to detect the OA level in mussel tissues by using streptavidin modified magnetic beads (Dominguez et al., 2012). In general, for bioassay MBs, they need to be chemically well designed to detect an analytical target. A varied of modified magnetic beads were applied to be an antibody carriers, which includes carboxyl or amino group functionalized beads (Dominguez et al., 2012; Jamshaid et al., 2016; Tetala & Vijayalakshmi, 2016), streptavidin-coated magnetic beads (Dominguez et al., 2012; Tetala & Vijayalakshmi, 2016), epoxy activated beads (Eissa et al., 2013; Iype et al., 2017; Schneck et al., 2016) and so on. Among here, the epoxy-functionalized process proved to be a superior approach, and epoxy-functionalized magnetic colloidal particles provided successful bioconjugation with biomolecules such as antibodies (Eissa et al., 2013). Schneck's report suggested the epoxy-functionalized microparticle performed slightly better than the amine-modified microparticles activated with glutaraldehyde (Schneck et al., 2016). Furthermore, epichlorohydrin was even directly used to entrap uncoated nanoparticles in a cross-linked matrix of protein, and the activity of the immobilized protein was not impaired (Iype et al., 2017).

In recent years, the carbon-shell magnetic beads have been reported and possessed several advantages of good biocompatibility, good hydrophilicity and versatile platform potentiality to be further modified (Deng et al., 2005; Qi, Lu, Deng, & Zhang, 2009; Wang, Bao, Wang, Zhang, & Li, 2006; Zhang, Duan, Li, & Lin, 2010). As a result of the abundant hydroxyl groups on the surface, carbon-shell magnetic beads (glycosylation modification) have promising potentiality to be activated by epoxy as facile immunological carries. However, there are fewer reports regarding the application of carbon-shell magnetic beads in the immunoassay field based on the ELISA approach, especially as an immunoassay carrier to analyse trace contamination in foodstuff. Thus, it is of great significance to exploit applying the feasibility of epoxy-activated Carbon-shell magnetic beads as immunoassay carrier in food safety analysis.

In this study, we developed epoxy groups functionalized Carbon-shell magnetic beads (MBs) and introduced them into rapid ELISA immunoassay procedures. Under magnetic field assistance provided by the magnetic bars integrated on the ELISA kit frame, the competitive immunoassay steps can be entirely accomplished in the same wells. In addition to the necessary characterization of MBs, the analytical performance of the currently presented analytical platform was evaluated by the detection of the marine toxin OA in shellfish.

## 2. Experimental section

### 2.1. Chemicals and materials

OA potassium salt, purchased from Jingqi Biotechnology Co. Ltd. (Wuxi, China), was first dissolved in DMSO ( $1.0 \text{ mg mL}^{-1}$ ) and then diluted in PBS ( $1\times$ , pH 7.4). Tween-20, HRP, BSA and casein were provided by Shanghai Leaf Source Biotechnology Co. Ltd (Shanghai, China). MAb-OA (JQ1501) and G-Mab (EKH303) were purchased from Jingqi Biotechnology Co. Ltd. (Wuxi, China). TMB was kindly provided by Key-Bio Biotech Co. Ltd. (Beijing, China). Polyethylene glycol (PEG-10000), glycol, epichlorohydrin and other common reagents were provided by National Drug Group Chemical Reagents Co. Ltd. (Shanghai, China). DTX-1, PSP, TTX, MC, NSP and ASP were purchased from Beacon Analytical Systems Inc. (Saco, USA). Ten milligrams of N-(3-dimethylaminopropyl)-N-ethyl-carbodiimide hydrochloride (EDC) and 5.0 mg of N-hydroxysuccinimide (NHS) were dissolved in 1.0 mL of 10.0 mM sodium acetate buffer as a crosslinking agent.

The dialysis membrane ( $\text{cutoff} = 20000$ ) was provided by Shanghai Leaf Source Biotechnology Co. Ltd. (Shanghai, China). The commercial ELISA kit for the analysis of OA was purchased from Beacon Analytical Systems Inc. (Saco, USA). The customized 96-well microplates integrated with insertable magnetic bars, were also kindly provided by Key-Bio Biotech Co. Ltd. (Beijing, China).

### 2.2. Apparatus

The morphologies of the fabricated MBs were observed using a Sirion-100 field-emitting scanning electron microscope (SEM, FEI, USA). The element analysis was analyzed by the auxiliary part EDX of Sirion-100. The entire ELISA measurements were performed by an ELISA microplate reader (FC, Thermo Fisher Life Sciences, China). A vortex-mixing device (IKA, Vibrax-VXR) was used for the sample extraction and whole assay process. As an alternative validation approach, OA analysis was performed by LC-MS/MS after separation with a  $C_{18}$  ( $100 \text{ mm} \times 2.1 \text{ mm} \times 2.6 \mu\text{m}$ , Phenomenex Kinetex) column and application to a Sciex Qtrap 4500 (AB Sciex, U.S.A.).

### 2.3. Preparation of magnetic beads and antibody immobilization

The formation of magnetic cores and fabrication of glycosylated magnetic beads were conducted with some modification of water thermal synthesis (Deng et al., 2005; Qi et al., 2009; Wang, Bao, Wang, Zhang, & Li, 2006; Zhang et al., 2010). The detailed information is provided in the supplementary materials. The final suspension of glycosylated magnetic beads was fixed at  $10.0 \text{ mg mL}^{-1}$  and maintained at  $4^\circ\text{C}$ .

Glycosylated MBs ( $20.0 \text{ mg}$ ) were transferred into a flask that contained  $20 \text{ mL}$  of NaOH solution ( $1.0 \text{ M}$ ), and then mixed completely with ultrasound dispersion. Twenty milliliters of epichlorohydrin and  $10 \text{ mL}$  of DMSO were added into the flask and mixed completely under stirring. The flask was set in a water bath ( $T = 45^\circ\text{C}$ ), and the whole reaction solution was stirred for  $4 \text{ h}$  at  $300 \text{ rpm min}^{-1}$ . The whole suspension was subsequently washed three times by ultrasonic washing with deionized water. Finally, the epoxy groups functionalized MBs (epoxy-MBs) were obtained and kept in DMSO at  $10.0 \text{ mg mL}^{-1}$ .

Epoxy-MBs dispersion (100  $\mu\text{L}$ ) at  $10.0 \text{ mg mL}^{-1}$  was rinsed with PBS buffer (1 $\times$ , pH = 7.4) three times. For antibody immobilization, a certain amount of G-Mab at  $1.0 \text{ mg mL}^{-1}$  (10–60  $\mu\text{L}$ ) was added to give a final volume of solution of 200  $\mu\text{L}$ . This mixed solution was maintained at  $37^\circ\text{C}$  for 1 h under gentle shaking, followed by washing 3 times with PBST (1 $\times$ , pH = 7.4, containing 0.05% Tween-20). After magnetic isolation, 1.0 mL of PBS (1 $\times$ , pH = 7.4) with 1.0% casein was used to block the unspecific site for 1 h. The final suspension of immunomagnetic beads had a concentration of  $1.0 \text{ mg mL}^{-1}$  and was maintained in PBS at  $4^\circ\text{C}$ . Besides, the routine ELISA microtiter plate for the OA comparative analysis for comparison was prepared as described in supplementary materials.

#### **2.4. Validation of epoxy groups on the MBs surface**

The density of the epoxy groups on the surface of the present MBs was determined by the sodium thiosulfate titration method and could be calculated according to the following equation (Teng, Sproule, Husain, & Lowe, 2000).

$$S = \frac{C_{\text{HCl}}(V_0 - V_1)}{m} \quad (1)$$

where  $S$  represents the density of epoxy groups ( $\mu\text{mol mg}^{-1}$ ),  $C_{\text{HCl}}$  is the concentration of hydrochloric acid, and  $V_0$  and  $V_1$  represent the consumption volume of hydrochloric acid with modified or unmodified by epoxy groups, respectively. Moreover,  $m$  was the mass of MBs (mg).

#### **2.5. Synthesis of OA-HRP conjugate**

OA standard solution 200  $\mu\text{L}$  at  $1.0 \text{ mg mL}^{-1}$  was added into the vessel that contained 20  $\mu\text{L}$  crosslinking agents and then mixed completely. Consequently, the coupling reaction was carried out for 30 min under gentle mixing. Then, 1.0 mL HRP solution ( $1 \text{ mg mL}^{-1}$  in 0.01 M PBS, pH 7.4) was added dropwise and gently mixed for 2 h. The solution was then maintained at  $4^\circ\text{C}$  overnight. The OA-HRP complex was subsequently purified by dialysis in PBS (1 $\times$ , pH = 7.4). During dialysis, the PBS (1 $\times$ , pH = 7.4) was changed 3 times. The final concentration of OA-HRP conjugate was kept at  $0.8 \text{ mg mL}^{-1}$ .

#### **2.6. The extraction of shellfish sample**

The extraction of the shellfish sample collected from Hangzhou bay was performed with reference to previous study (Su et al., 2017). Two grams of a homogenate of the edible part of shellfish was weighed into a 50 mL plastic vessel and spiked with OA solution. Ten milliliters of methanol/water (80/20) were added into the vessel and continuously mixed for 5 min. After centrifugation at  $5000 \text{ rpm min}^{-1}$  for 10 min, 1.0 mL of the supernatant was filtered through a  $0.45 \mu\text{m}$  microporous membrane and then dissolved in 9.0 mL of PBS (1 $\times$ , pH = 7.4) for analysis.

## 2.7. Competitive immunoassay and colorimetric measurements

Prior to the assay, all test wells of the blank microplate had been saturated by 1.0% BSA solution for 1 h. First, 10.0  $\mu\text{L}$  of the G-Mab-MBs ( $1.0 \text{ mg mL}^{-1}$ ) was added into each well of a blank microplate that contained 100  $\mu\text{L}$  of PBS buffer. Afterwards, 100  $\mu\text{L}$  of OA standard solutions at different concentrations or sample extraction solution, 50  $\mu\text{L}$  diluted OA-HRP solution and 50  $\mu\text{L}$  diluted monoclonal antibody solution were added. After covering with parafilm, the test 96-well plate was closed with a plastic cap and fixed with two foldback clips. All wells were gently vortex-mixed, and the assays were maintained for 40 min under  $30^\circ\text{C}$ . The test microplates were then installed onto the base plate with magnetic bars to isolate MB nanoparticles onto the inner wall in each well. After several cycles of rinsing and magnetic isolation, the residual MBs in the 96-wells were mixed with 100  $\mu\text{L}$  of TMB solution and incubated for 15 min at room temperature ( $25^\circ\text{C}$ ). Finally, magnetic isolation was again performed, and the colorimetric assay was stopped with stop solution.

The detection wavelengths were set at 450 and 620 nm under the dual wavelength mode. The OD value was calculated in the equation  $\text{OD} = \text{OD}_{450} - \text{OD}_{620}$ . The IR was also calculated to determine the OA concentration in the samples, according to the equation as follows.

$$\text{IR} = \frac{A_0 - A_1}{A_0 - A_{\text{blank}}} * 100\% \quad (2)$$

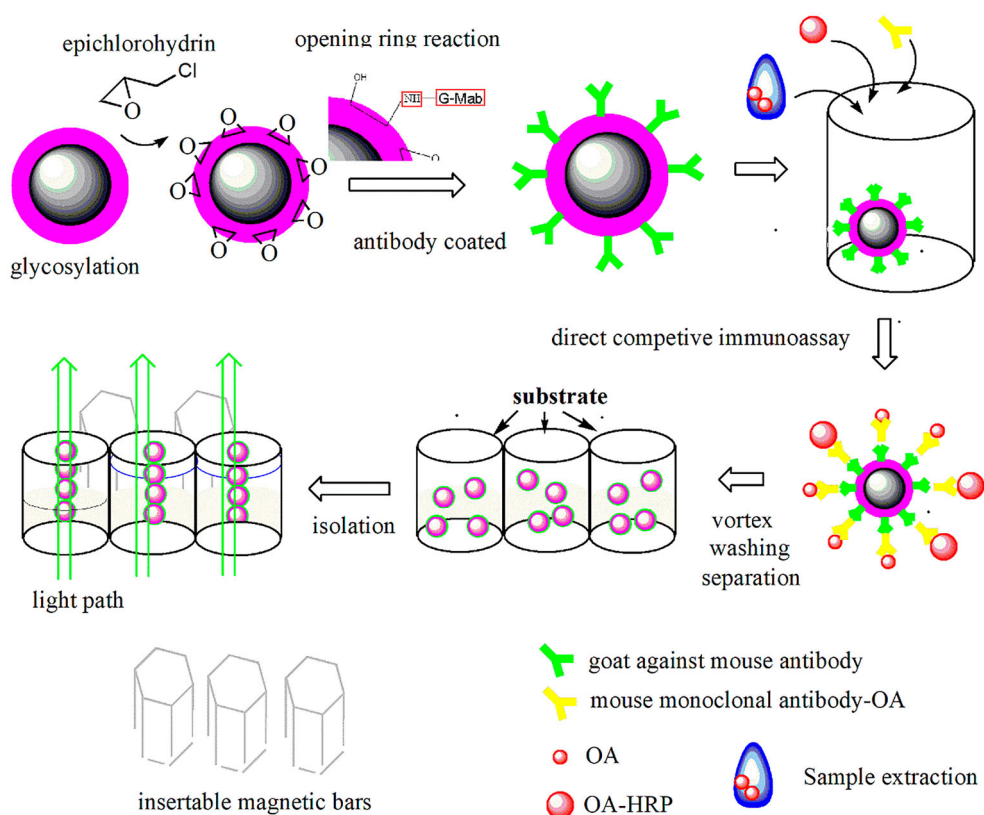
where IR represents the inhibitory content of sample extraction competitive binding with antibody against enzyme labelled antigen conjugate and  $A_0$  is the OD of the standard or sample solution without antigen.  $A_1$  is the OD of the standard or sample solution with antigen.  $A_{\text{blank}}$  is the average OD of the testing solution without antigen and enzyme-labelled conjugate. The entire scheme of the fabrication of MBs and the current ELISA approach under magnetic field assistance are shown in [Scheme 1](#), and the structure of the 96-well microplate integrated with magnetic bars is shown in Fig. 1S of the supplementary materials.

## 2.8. Interference, cross-reactive test

Six types of algal toxins, including STX, TTX, GTX2&3, MC, ASP, and DTX-1, were selected as substrates to evaluate interference and cross reactivity. The interference concentrations of these six types of toxins were investigated from 0.78 to  $50.0 \mu\text{g L}^{-1}$ . Within it, DTX-1 is considered a natural derivative compound of OA, thus, the  $\text{IC}_{50}$  of DTX-1 was performed at different concentrations ranging from 0.78 to  $50.0 \mu\text{g L}^{-1}$  for comparison. Different levels of OA (from 0.39 to  $25.0 \mu\text{g L}^{-1}$ ) were also simultaneously prepared to calculate the  $\text{IC}_{50}$  to estimate the immunoassay cross-reactivity (CR, %) with DTX-1, and all CR values were listed in the inserted table of [Figure 2](#).

## 2.9. Recovery tests, real sample test and validation

To validate the ruggedness of our established method, the recovery of OA in spiked samples was carried out via a Beacon kit and HPLC-MS/MS analysis, the relevant analytical parameters and procedures were referred according to concerned method with part



**Scheme 1.** The rapid competitive ELISA assay based on the epoxy-magnetic beads protocol.

modification (McNabb, Selwood, & Holland, 2005). The spiked concentrations in the shellfish samples (blank samples had been verified by LC-MS/MS) were at 50.0, 100.0, and 300.0  $\mu\text{g kg}^{-1}$ , respectively. In addition, the correlation of the results between the presented immunomagnetic beads approach and the HPLC-MS/MS method was also investigated.

### 3. Results and discussion

#### 3.1. The characterization of varied modification of MBs

Fabricated glycosylated magnetic beads were characterized by scanning electron microscopy (SEM) and energy dispersive X-ray spectrometry (EDX). According to the SEM image in Figure 1, the surfaces of the bare magnetic bead cores were smooth and uniform (Figure 1(A)), however, the rougher surfaces of the glycosylated magnetic beads were observed (Figure 1(B)). Furthermore, the EDX element analysis presented an obvious C element peak in the insert chart of Figure 1(B) by comparison of the insert of Figure 1(A). These results implied that the present modified bead surface was coated with a layer of carbon-shell from glucose deposition. Moreover, the average diameter of the MBs encapsulated with a glycosylation base in this study was estimated at 800

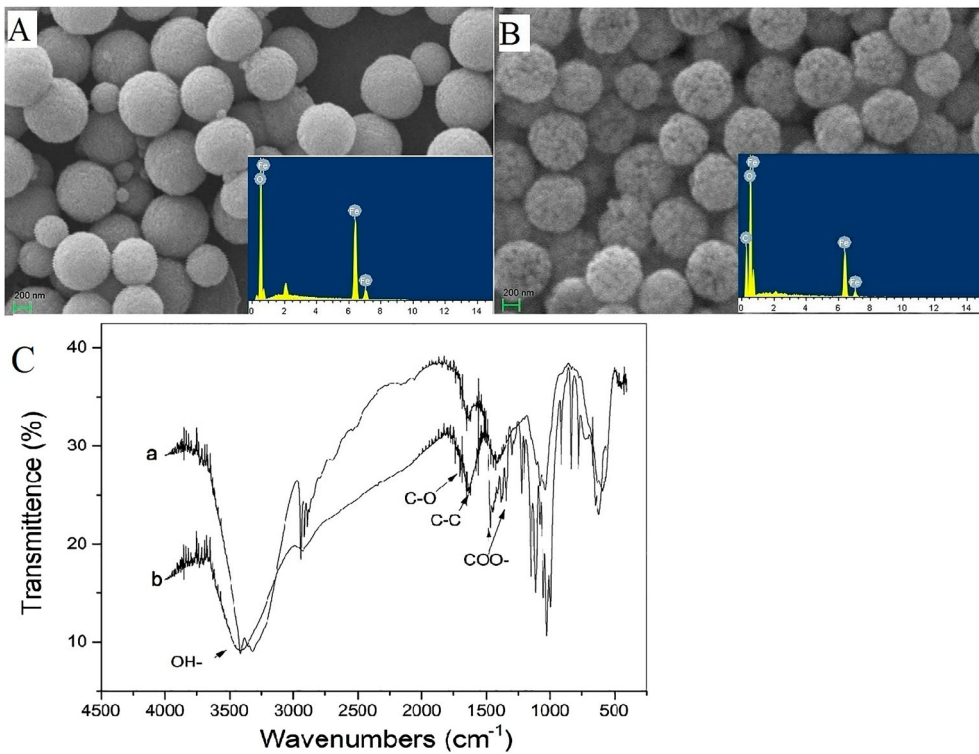


**Figure 1.** The morphology of bare magnetic beads and glycosylated beads, EDX profiles and Fourier transform infrared (FTIR) characterization (A) The SEM and EDX profiles of bare magnetic beads (B) The SEM and EDX profiles of glycosylated beads. (C) FTIR spectra of the glucose and glycosylated MBs samples: a-glucose b-glycosylated MBs.

nm, which could be considered an ideal candidate for immunoassay carrier materials, in comparison with the common commercial immunoassay MBs that have a diameter of nearly  $1.0\ \mu\text{m}$ .

On the other hand, under appropriate hydrothermal treatment conditions, glucose molecules can be deposited and transformed to be a layer of complicate polymer and carbonization structure. Previous studies suggested that the carbon shell microspheres have a core-shell chemical structure, which contains a high density of reactive/hydrophilic oxygen functional groups (including hydroxyl, phenolic, carbonyl, carboxylic, and ester) (Sevilla & Fuertes, 2009; Sun & Li, 2004). Full coverage of the derived polymer of glucose suggested that the modified MBs in this study were with abounding hydrophilic groups and, thus, had a good hydrophilic performance in aqueous solution. The glycosylated MBs produced good dispersion and absorption abilities in aqueous solution (Yang et al., 2011; Zhang & Kong, 2011). Furthermore, the infrared spectra of carbon-shell MBs and glucose also indicated the residual groups presence of saccharide compounds on the coating layer of the present MBs (see Figure 1(C)), and the concerned groups have also been marked in this figure (Sun & Li, 2004). Therefore, the encapsulation of MBs with natural or artificial polymers from saccharides might be endowed with the advantages of good biocompatibility, colloidal stability in aqueous and physiological

media. Given these considerations above, the present glycosylation carbon-shell MBs appear promising candidate carriers for bioassay.

### **3.2. The principle of epoxy functionalization**

In general, the covalent coupling method is a routine linking approach between an antibody and a carrier's surface such as MBs, microspheres, and resin. Any ligand with free primary amine groups, such as the  $\epsilon$ -amine group of proteins or antibodies, can be attached directly attached to the epoxy functionalized matrix, thus, the approach of coupling epoxy groups has been verified to be an effective immobilization strategy (Schneck et al., 2016). Considering glycosylated MBs in our current work abounding with the high density of hydroxyl groups, it was achievable for the functional modification of the epoxy groups in aqueous solution. According to the sodium thiosulfate titration method, the epoxy-density of MBs in this study was calculated to be  $71.5 \text{ mmol g}^{-1}$  (wet weight MB). Compared with the epoxy-activated gel ( $50 \text{ mmol g}^{-1}$  wet weight gel) for chromatography separation (Teng et al., 2000), our results suggested that the epoxy-MBs exhibited a higher epoxy group's density.

The immunological activity of the fabricated G-Mab-MBs in this study was also investigated. Briefly, 10 mg G-Mab- or BSA-modified MBs of the control group were simultaneously introduced inside the wells of microplates, followed by the addition of 50  $\mu\text{L}$  MAb (1:8000 diluted, reserved concentration is  $2.0 \text{ mg mL}^{-1}$ ) and 50  $\mu\text{L}$  OA-HRP conjugate solution (1:8000 diluted reserved OA-HRP conjugates). The results showed that the G-Mab-MBs exhibited a high affinity towards MAb-OA, with an absolute absorbance value of 3.241 (over the linear range of the current instrument). However, the MBs control group modified only by BSA generated an absolute absorbance of 0.02, which implies that the G-Mab coating is the preliminary condition to form the complex of MAb and OA-HRP on the surface of MBs. Thus, it was observed by the substrate colour reaction leading to a conclusion that the epoxy functionalized MBs successfully coupled with G-Mab and maintained their immunological activity.

### **3.3. Operational advantages of the analytical platform**

To simplify operational parameters and effectively enhance the reproducibility of tests of this ELISA protocol, the employment of MBs brought these operational advantages as expected. As the immunoassay and colorimetric steps present good performance, the reproducibility of the analysis is confirmed. The current magnetic field provides a simple operational platform to accomplish competitive immunoassay procedures. Moreover, the fabricated immunological MBs did not produce observable fouling on the inner wall of each well, which is rationally beneficial to the following re-dispersion process. Attributed to the magnetic bars, the rinse of every step is easily operated and congregated MBs on the inner wall without interrupting the light path during detection. Therefore, based on these operational advantages above, the matrix effect was also minimized and the total reaction time cost decreased to less than 60 min.

### 3.4. The optimization of concerned assay parameters

Several parameters concerning the immunoassay were investigated in this study, including the coating amount of G-Mab, coating time, the amount of immunomagnetic beads, dilution fold of OA-HRP conjugate and MAb. Here, the  $OD_{max}$ ,  $OD_{blank}$  and their ratio of them were used as the optimization index of these parameters.

At first, appropriate amount of G-Mab coating on the MBs was an assurance for following immunoassay. The  $OD_{max}$  increased with the increase of coating amount of G-Mab, as shown in Fig. 2S-A of supplementary materials. However, when the coating amount reached 30  $\mu\text{g}$ , the OD value was 1.19 and there was no longer an obvious increase. This phenomenon implied the active sites of the epoxy-MBs might be saturated. Thus, the optimum coating amount of G-Mab was selected to be 30  $\mu\text{g}$  as for 1.0 mg epoxy-MBs. Moreover, the optimization test of the coating time was performed, and the maximum OD value occurred at 40 min. On the other hand, Fig. 2S-B demonstrates the optimum amount of immunological MBs in the present approach. With the increase of the use amount of immunomagnetic bead, the  $OD_{blank}$  and  $OD_{max}$  values in the blank simultaneously increased, however, the  $OD_{max}/OD_{blank}$  value showed a decreasing tendency. This finding could be attributed to the nonspecific absorbance after excessive MB usage. Therefore, the use of 10  $\mu\text{g}$  of MBs (10  $\mu\text{L}$ , 1.0 mg  $\text{mL}^{-1}$ ) was sufficient for the following assay.

Furthermore, throughout the crossover design, the optimum dilution ratios of OA-HRP and MAb used in the homogenous phase assay have also been carefully considered. The OD value was used as the optimization index of these parameters and the expected absorbance of the immunoassay colorimetric solution was located in the range of 0.9–1.0. After screening microtiter wells, the immunoassay colorimetric results represented the best response when OA-HRP and OA monoclonal antibody were equally diluted at 1:16000 or OA-HRP was diluted at 1:8000 and OA MAb at 1:32000 (shown in the Table 1S of the supplementary materials). Furthermore, for the comparison of the binding standard curves of the two combinations, the linearity and slope of the combination of OA-HRP (1:8000) and OA MAb (1:32000) gave better analytical performance (figure not shown). Moreover, MAb diluted at 1:32000 further decreased the preparation cost of the current fabricated kit. Thus, the following experiments were carried out based on the ratio of OA-HRP (1:8000) and OA MAb (1:32000).

### 3.5. Cross-reactivity and interference test

To investigate the specific interaction between MAb, free OA or OA-HRP conjugate and immunomagnetic beads in a homogenous solution of each well, potential interferences including paralytic shellfish (e.g. ASP), DSP (e.g., DTX-1) and other algal toxins were investigated. The results of the cross reaction and interference test are shown in the Figure 2. The interference effects did not occur between OA and the other shellfish toxins except for DTX-1. First, as shown in the insert table of Figure 2, not detectable cross reactivity can be found nearly all algal toxins (25.0  $\mu\text{g L}^{-1}$ ) except for DTX-1.

However, DTX-1 provided obvious cross-reactivity, which produced nearly 40% CR value (refer to the insert table of Figure 2). It is generally accepted that the OA toxins were a group of fat soluble, heat stable polyether compounds, which include OA and

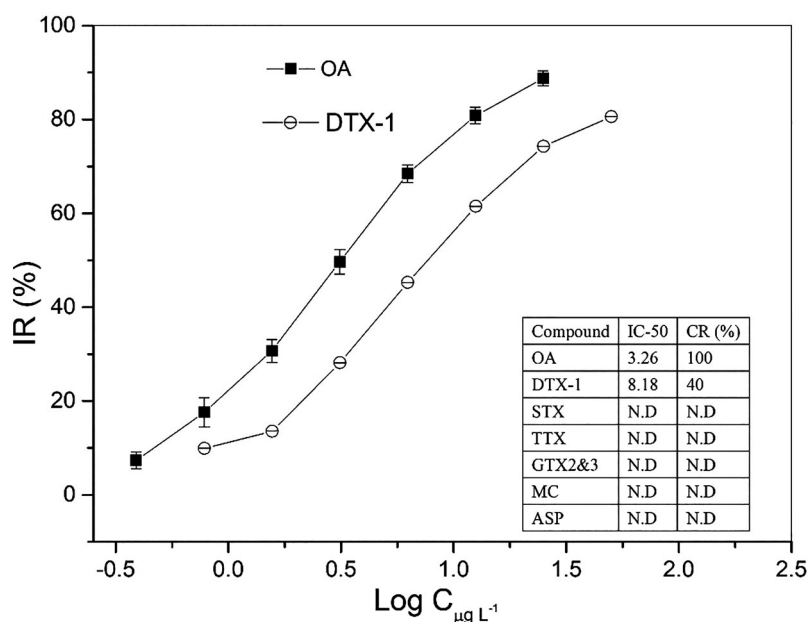


**Figure 2.** Cross-reactivity under the coexistence of other interferences. The  $IC_{50}$  investigation for OA ranged from 0.39 to 25.0  $\mu\text{g L}^{-1}$ , and DTX-1 ranged from 0.78 to 50.0  $\mu\text{g L}^{-1}$ . The assay condition of insert table consisted of the interfering substance at a concentration of 25.0  $\mu\text{g L}^{-1}$ .

structural analogues referred to as dinophys toxins (DTXs). DTX-1 had an additional methyl group (35-methyl-OA, see Fig. 3S of supplementary materials) and produces an assured colorimetric reaction under the current immunoassay approach. Due to the unavoidable cross-activity effects, it was reported that toxicity equivalency factors (TEFs) were assigned equally for OA and DTX-1 (Jawaid et al., 2015). Despite this existence of cross-reactivity, in this study, we should note that the  $IC_{50}$  of DTX-1 is 8.18  $\mu\text{g L}^{-1}$ , which is higher than the value of 3.26  $\mu\text{g L}^{-1}$  of OA, equal to the value of 160  $\mu\text{g kg}^{-1}$  in a real sample. Jawaid and coworkers reported that samples containing at or greater than 160  $\mu\text{g kg}^{-1}$  will generate noncompliant results, and a 95% accuracy level at correctly identifying 60  $\mu\text{g kg}^{-1}$  samples as compliant was observed in a lateral flow immunoassay study (Jawaid et al., 2015). The results from naturally contaminated samples indicated no false compliant results and no false noncompliant results at <50% MPL (OA is 160  $\mu\text{g kg}^{-1}$ ), and these results implied that the DTX-1 will not produce obvious interference in the OA analysis, especially at the lower level of OA in real samples. With considerations of the availability of rational dilution of sample extraction containing a high level of OA, the present OA analysis strategy still demonstrated good specificity.

### 3.6. The analytical performance and stability

For immunoassay, the half maximal inhibitory concentration- $IC_{50}$  represents the concentration of an inhibitor or competitor that will produce a 50% IR value of immunoassay such as enzyme labelled antigen or antibody. It is commonly used as a measurement parameter of ELISA analysis. Based on the optimized experimental conditions, the current

designed immunomagnetic beads demonstrated promising analytical potentiality. For competition assays, 10% IR value corresponding concentration can be considered as a LOD in the screening test (Hayat, Barthelmebs, & Marty, 2011). The correlation coefficient  $R$ , the  $IC_{50}$  and LOD values derived from the regression equation were shown in the Figure 3. Using the current approach to detect the OA concentration provided a good linear relationship in the range of  $0.35\text{--}25.0\ \mu\text{g L}^{-1}$  with a half maximal inhibitory concentration  $IC_{50} = 3.27\ \mu\text{g L}^{-1}$  and LOD values of  $0.35\ \mu\text{g L}^{-1}$ . However, the comparative routine ELISA kit without the participation of MBs offered  $IC_{50} = 4.37\ \mu\text{g L}^{-1}$  with LOD  $0.82\ \mu\text{g L}^{-1}$ . Thus, the LOD and  $IC_{50}$  of the present MB protocol have been improved. Furthermore, the operational process was significantly simplified. The improved analytical performance of the current established approach can be attributed to the employment of immunological MBs as carriers and that the entire immunoassay occurred in a homogeneous solution. MBs as biological supporting carriers could provide a large binding surface area, which could enable the proper orientation of the antibody binding sites, improving the sensitivity of immunoassays (Hayat et al., 2011; Johnson, Harrison, & Turner, 2016). In this study, the epoxy group functionalized MBs provided abundant sites for the immobilization of G-Mab, and all competitive steps happened in homogenous phase and formed immune complex should combined with the immunological sites of G-Mab-MBs finally. Therefore, it was believed that the current established protocol effectively assured the proper orientation and binding sites between G-Mab and MAb. Similarly, Hayat and co-workers reported that the introduction of protein-G-MBs effectively increase the sensitivity of the analytical system as compared to antibody physical adsorption based detection (Hayat et al., 2012).

On other hand, to further disclose the analytical performance of the currently established MB assisted competitive ELISA approach, a comparison of relevant analytical

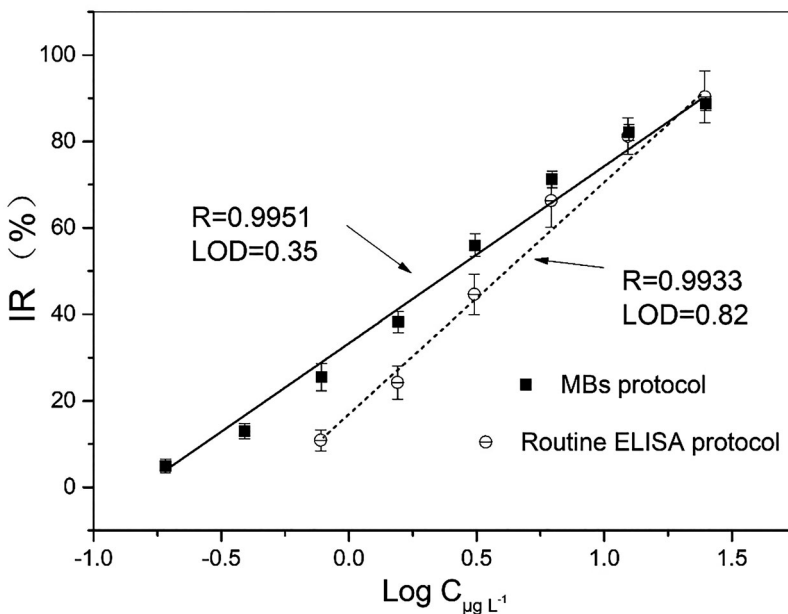


**Figure 3.** Calibration curves of the presented MB protocol, routine ELISA protocol.

parameters based on a competitive immunoassay performed with MB assistance during past decade has been investigated, and the results are listed in Table 1 (Dominguez et al., 2012; Hayat et al., 2011, 2012; Johnson et al., 2016; Lu et al. 2012; Pan et al., 2018). Briefly, our results demonstrated the advantages displayed by the use of immunomagnetic beads with providing short interaction time between the antibody and the target, thus enhancing the performance of the developed ELISA. Presented ELISA approach based on epoxy-functionalized immunomagnetic beads demonstrated operational and analytical advantages with lower LOD and wider linear range over other reported ELISA protocol, although some reported immunosensor possessed very high sensitivity.

### 3.8. The recovery test of spiked samples

The recovery results for the current MB approach validated the reliability of the methods at three different spiking levels of 50.0, 100 and 300  $\mu\text{g kg}^{-1}$ , which are concentrations of OA that are lower or higher than the highest level allowed by the European Commission (160  $\mu\text{g kg}^{-1}$ ) (Commission Regulation (EC) No. 853/2004). The recovery results analyzed by three different protocols are shown in Table 2.

The precision was determined by the relative standard deviation (% RSD) for the quartic measurements. The results showed that the recovery level (%) obtained is in

**Table 1.** The analytical performance comparison of relevant works.

Number	Type	LOD ( $\mu\text{g L}^{-1}$ )	IC <sub>50</sub> ( $\mu\text{g L}^{-1}$ )	Linear range ( $\mu\text{g L}^{-1}$ )	ELISA strategy
1	Immunosensor	0.15	/	0.19–25	Immunosensor with streptavidin-MBs Indirect competitive [Dominguez et al., 2012]
2	Immunosensor	0.05	/	0.2–20	Fluorescence immunosensor with streptavidin-MBs. Indirect competitive [Pan et al., 2018]
3	ELISA kit	0.45	4.4	0.4–12.5	Routine ELISA kit, Indirect competitive [Lu et al., 2012]
4	ELISA kit	1.0	/	1.0–90	ELISA with protein G-MBs. Direct competitive [Hayat et al., 2012]
5	ELISA kit	31.3 $\mu\text{g OA eq/kg}^a$	/	31.3–1703 $\mu\text{g OA eq/kg}$	Routine ELISA kit, Direct competitive [Johnson et al., 2016]
6	ELISA kit	0.8	3.92	/	ELISA with Streptavidin-MBs. indirect competitive [Hayat et al., 2011]
7	ELISA kit	0.35 <sup>b</sup>	3.27	0.35–25.0 <sup>c</sup>	ELISA with epoxy-MBs direct competitive [this work]

<sup>a</sup>OA equivalents- OA eq.

<sup>b</sup>Equally to 17.5  $\mu\text{g kg}^{-1}$  in 2.0 g of sample.

<sup>c</sup>Equally to 17.5–1250  $\mu\text{g kg}^{-1}$ .

**Table 2.** The spiking tests and recovery results ( $n = 4$ ).

Item/number	Spiking level (50.0 $\mu\text{g kg}^{-1}$ )		Spiking level (100.0 $\mu\text{g kg}^{-1}$ )		Spiking level (300.0 $\mu\text{g kg}^{-1}$ )	
	Result ( $\mu\text{g kg}^{-1}$ )	Recovery Rate (%)	Result ( $\mu\text{g kg}^{-1}$ )	Recovery Rate (%)	Result ( $\mu\text{g kg}^{-1}$ )	Recovery Rate (%)
Averages $\pm$ SD <sup>a</sup>	48.28 $\pm$ 5.36	96.56 $\pm$ 10.72	97.93 $\pm$ 7.81	97.93 $\pm$ 7.81	307.5 $\pm$ 15.7	102.5 $\pm$ 5.23
CVs	11.09		7.98		5.12	

<sup>a</sup>Quartic analysis for every spiking level.

**Table 3.** Comparison of real sample detection within the three kinds of approaches ( $n = 4$ ).

Samples	Detection results ( $\mu\text{g kg}^{-1}$ ) Mean $\pm$ SD <sup>a</sup>			
	MBs approach	Commercial ELISA Kits	HPLC-MS/MS	
Sinonovacula Constricta	–01	17.56 $\pm$ 3.24	N.D <sup>b</sup>	15.46 $\pm$ 1.35
	–02	N.D	N.D	8.81 $\pm$ 1.17
	–03	N.D	N.D	N.D
Pectinid	–01	N.D	N.D	11.45 $\pm$ 1.02
	–02	N.D	N.D	N.D
	–03	N.D	N.D	N.D
Mytilus Coruscus	–01	54.67 $\pm$ 5.67	57.23 $\pm$ 6.24	46.37 $\pm$ 4.35
	–02	32.17 $\pm$ 2.45	N.D	25.17 $\pm$ 2.74
	–03	N.D	N.D	N.D

<sup>a</sup>Analysis for every real sample ( $n = 4$ ).<sup>b</sup>No detection.

good agreement with the spiked amount of OA. It can be found that the recovery rates ranged between 96.56% and 102.5%. Moreover, the CV values ranged from 5.12% to 11.09% which is lower than 15%, suggesting the current established protocol is robust and reliable.

### 3.9. The real analysis and validation

In addition to recovery tests, real samples collected from local aquatic farms and wild fishery harvested in Zhejiang province that have been tested based on the current MB approach, commercial ELISA Beacon kit and HPLC-MS/MS method, respectively. The comparisons of the analysis results based on the three types of methods are listed in Table 3. The real analytical data demonstrated that the performance of the current MB approach in this study is reliable and as good as the LC-MS/MS and commercial kit performance. Moreover, the linear correlation of the analysis results between the current MB approach and the HPLC-MS/MS method was higher than 0.9 ( $R^2 = 0.961$ ), which, again, implied the results based on the current approach were reliable (seen in Fig. 4S).

## 4. Conclusions

This work reported the fabrication of epoxy group-activated MBs and their application in the rapid ELISA analysis of the marine toxin okadaic acid. Under magnetic field assistance, the present established protocol can achieve high sensitivity, easy-operation, rapid and reliable ELISA detection of OA. The constructed epoxy carbon-shell MBs played a role as a versatile and biocompatible carrier for antibody immobilization and also demonstrated a rapid magnetic response, rapid re-dispersion, and easy-operational behaviours for immune assays. The experiments with real samples validated the reliability of the present immunoassay for OA detection. The results obtained with this method are comparable to the routine commercial ELISA kit in terms of the sensitivity and analytical linear range. Moreover, the significant labours required have been decreased due to the introduction of MBs and magnetic field assistant slots. Thus, the presently established ELISA method, with the aid of magnetic fields, can be an alternative strategy to the conventional assays for OA detection. The developed approach was rapid, simple and cost-effective, which also demonstrated the promise of epoxy carbon-shell MB application for the development of novel biosensing analytical protocols in the future.

## Disclosure statement

No potential conflict of interest was reported by the authors.

## Funding

This study has been financially supported by Research project on public welfare Technology of Zhejiang province (2016C32082) and (LGF18C200006).

## ORCID

Yiming Zhang  <http://orcid.org/0000-0003-4356-7245>

## References

- Agrawal, A., Sathe, T., & Nie, S. (2007). Single-bead immunoassays using magnetic microparticles and spectral-shifting quantum dots. *Journal of Agricultural and Food Chemistry*, 55(10), 3778–3782.
- Deng, H., Li, X. L., Peng, Q., Wang, X., Chen, J. P., & Li, Y. D. (2005). Monodisperse magnetic single-crystal ferrite microspheres. *Angewandte Chemie-International Edition*, 44(18), 2782–2785.
- Dominguez, R. B., Hayat, A., Sassolas, A., Alonso, G. A., Munoz, R., & Marty, J. L. (2012). Automated flow-through amperometric immunosensor for highly sensitive and on-line detection of Okadaic acid in mussel sample. *Talanta*, 99, 232–237.
- Eissa, M. M., Rahman, M. M., Zine, N., Jaffrezic, N., Errachid, A., Fessi, H., & Elaissari, A. (2013). Reactive magnetic poly(divinylbenzene-co-glycidyl methacrylate) colloidal particles for specific antigen detection using microcontact printing technique. *Acta Biomaterialia*, 9(3), 5573–5582.
- Garthwaite, I., Ross, K. M., Miles, C. O., Briggs, L. R., Towers, N. R., Borrell, T., & Busby, P. (2001). Integrated enzyme-linked immunosorbent assay screening system for amnesic, neurotoxic, diarrhetic, and paralytic shellfish poisoning toxins found in New Zealand. *Journal of Aoac International*, 84(5), 1643–1648.
- Hayat, A., Barthelmebs, L., & Marty, J.-L. (2011). Enzyme-linked immunosensor based on super paramagnetic nanobeads for easy and rapid detection of Okadaic acid. *Analytica Chimica Acta*, 690(2), 248–252.
- Hayat, A., Barthelmebs, L., Sassolas, A., & Marty, J.-L. (2012). Development of a novel label-free amperometric immunosensor for the detection of Okadaic acid. *Analytica Chimica Acta*, 724, 92–97.
- Iype, T., Thomas, J., Mohan, S., Johnson, K. K., George, L. E., Ambattu, L. A., ... Ramchand, C. N. (2017). A novel method for immobilization of proteins via entrapment of magnetic nanoparticles through epoxy cross-linking. *Analytical Biochemistry*, 519, 42–50.
- Jamshaid, T., Tenorio Neto, E. T., Eissa, M. M., Zine, N., Kunita, M. H., El-Salhi, A. E., & Elaissari, A. (2016). Magnetic particles: From preparation to lab-on-a-chip, biosensors, microsystems and microfluidics applications. *Trac-Trends in Analytical Chemistry*, 79, 344–362.
- Jawaid, W., Meneely, J. P., Campbell, K., Melville, K., Holmes, S. J., Rice, J., & Elliott, C. T. (2015). Development and validation of a lateral flow immunoassay for the rapid screening of Okadaic acid and all dinophysins toxins from shellfish extracts. *Journal of Agricultural and Food Chemistry*, 63(38), 8574–8583.
- Johnson, S., Harrison, K., & Turner, A. D. (2016). Application of rapid test kits for the determination of diarrhetic shellfish poisoning (DSP) toxins in bivalve molluscs from Great Britain. *Toxicon*, 111, 121–129.

- Kolosova, A. Y., Shim, W. B., Yang, Z. Y., Eremin, S. A., & Chung, D. H. (2006). Direct competitive ELISA based on a monoclonal antibody for detection of aflatoxin B-1. Stabilization of ELISA kit components and application to grain samples. *Analytical and Bioanalytical Chemistry*, 384(1), 286–294.
- Li, H., Xiya, S., Zhang, X., Li, C., Dong, B., Mujtaba, M. G., ... Wang, Z. (2018). Generic Hapten synthesis, broad-specificity monoclonal antibodies preparation, and ultrasensitive ELISA for five antibacterial synergists in chicken and milk. *Journal of Agricultural and Food Chemistry*, 66(42), 11170–11179.
- Lin, C., Liu, Z.-S., Tan, C.-Y., Guo, Y.-P., Li, L., Ren, H.-L., ... Lu, S.-Y. (2015). Contamination of commercially available seafood by key diarrhetic shellfish poisons along the coast of China. *Environmental Science and Pollution Research*, 22(2), 1545–1553.
- Lin, C., Liu, Z.-S., Wang, D.-X., Ren, H.-L., Li, Y.-S., Hu, P., ... Lu, S.-Y. (2014). Sensitive and reliable micro-plate chemiluminescence enzyme immunoassay for Okadaic acid in shellfish. *Analytical Methods*, 6(18), 7142–7148.
- Liu, B.-H., Hung, C.-T., Lu, C.-C., Chou, H.-N., & Yu, F.-Y. (2014). Production of monoclonal antibody for Okadaic acid and its utilization in an ultrasensitive enzyme-linked immunosorbent assay and one-step Immunochromatographic strip. *Journal of Agricultural and Food Chemistry*, 62(6), 1254–1260.
- Llamas, N. M., Stewart, L., Fodey, T., Higgins, H. C., Velasco, M. L. R., Botana, L. M., & Elliott, C. T. (2007). Development of a novel immunobiosensor method for the rapid detection of Okadaic acid contamination in shellfish extracts. *Analytical and Bioanalytical Chemistry*, 389(2), 581–587.
- Lu, S.-Y., Lin, C., Li, Y.-S., Zhou, Y., Meng, X.-M., Yu, S.-Y., ... Liu, Z.-S. (2012). A screening lateral flow immunochromatographic assay for on-site detection of Okadaic acid in shellfish products. *Analytical Biochemistry*, 422(2), 59–65.
- Lu, S.-Y., Zhou, Y., Li, Y.-S., Lin, C., Meng, X.-M., Yan, D.-M., ... Ren, H.-L. (2012). Production of monoclonal antibody and application in indirect competitive ELISA for detecting Okadaic acid and dinophytotoxin-1 in seafood. *Environmental Science and Pollution Research*, 19(7), 2619–2626.
- McNabb, P., Selwood, A. I., & Holland, P. T. (2005). Multiresidue method for determination of algal toxins in shellfish: Single-laboratory validation and interlaboratory study. *Journal of Aoac International*, 88(3), 761–772.
- Pan, Y., Wei, X., Liang, T., Zhou, J., Wan, H., Hu, N., & Wang, P. (2018). A magnetic beads-based portable flow cytometry immunosensor for in-situ detection of marine biotoxin. *Biomedical Microdevices*, 20, 3.
- Paredes, I., Rietjens, I. M. C. M., Vieites, J. M., & Cabado, A. G. (2011). Update of risk assessments of main marine biotoxins in the European Union. *Toxicon*, 58(4), 336–354.
- Pleadin, J., Vulic, A., Persi, N., Skrivanko, M., Capek, B., & Cvetnic, Z. (2014). Aflatoxin B-1 occurrence in maize sampled from Croatian farms and feed factories during 2013. *Food Control*, 40, 286–291.
- Prassopoulou, E., Katikou, P., Georgantelis, D., & Kyritsakis, A. (2009). Detection of Okadaic acid and related esters in mussels during diarrhetic shellfish poisoning (DSP) episodes in Greece using the mouse bioassay, the PP2A inhibition assay and HPLC with fluorimetric detection. *Toxicon*, 53(2), 214–227.
- Qi, D., Lu, J., Deng, C., & Zhang, X. (2009). Magnetically responsive Fe<sub>3</sub>O<sub>4</sub>@C@SnO<sub>2</sub> core-shell microspheres: Synthesis, characterization and application in phosphoproteomics. *Journal of Physical Chemistry C*, 113(36), 15854–15861.
- Radoi, A., Targa, M., Prieto-Simon, B., & Marty, J. L. (2008). Enzyme-linked immunosorbent assay (ELISA) based on superparamagnetic nanoparticles for aflatoxin M-1 detection. *Talanta*, 77(1), 138–143.
- Schneck, N. A., Phinney, K. W., Lee, S. B., & Lowenthal, M. S. (2016). Quantification of antibody coupled to magnetic particles by targeted mass spectrometry. *Analytical and Bioanalytical Chemistry*, 408(29), 8325–8332.
- Sevilla, M., & Fuertes, A. B. (2009). Chemical and structural properties of carbonaceous products obtained by hydrothermal carbonization of saccharides. *Chemistry-a European Journal*, 15(16), 4195–4203.

- Stengel, D. B., & Connan, S. (2015). Marine Algae: A source of biomass for biotechnological applications. *Natural Products From Marine Algae: Methods and Protocols*, 1308, 1–37.
- Su, K., Qiu, X., Fang, J., Zou, Q., & Wang, P. (2017). An improved efficient biochemical detection method to marine toxins with a smartphone-based portable system-Bionic e-Eye. *Sensors and Actuators B-Chemical*, 238, 1165–1172.
- Suganuma, M., Fujiki, H., Suguri, H., Yoshizawa, S., Hirota, M., Nakayasu, M., ... Sugimura, T. (1988). Okadaic acid-an additional non-phorbol-12-tetradecanoate-13-acetate-type tumor promoter. *Proceedings of the National Academy of Sciences of the United States of America*, 85(6), 1768–1771.
- Sun, X. M., & Li, Y. D. (2004). Colloidal carbon spheres and their core/shell structures with noble-metal nanoparticles. *Angewandte Chemie-International Edition*, 43(5), 597–601.
- Teng, S. F., Sproule, K., Husain, A., & Lowe, C. R. (2000). Affinity chromatography on immobilized “biomimetic” ligands synthesis, immobilization and chromatographic assessment of an immunoglobulin G-binding ligand. *Journal of Chromatography B-Analytical Technologies in the Biomedical and Life Sciences*, 740(1), 1–15.
- Tetala, K. K. R., & Vijayalakshmi, M. A. (2016). A review on recent developments for biomolecule separation at analytical scale using microfluidic devices. *Analytica Chimica Acta*, 906, 7–21.
- Wang, L. Y., Bao, J., Wang, L., Zhang, F., & Li, Y. D. (2006). One-pot synthesis and bioapplication of amine-functionalized magnetite nanoparticles and hollow nanospheres. *Chemistry-a European Journal*, 12(24), 6341–6347.
- Wang, X., Niessner, R., Tang, D. P., & Knopp, D. (2016). Nanoparticle-based immunosensors and immunoassays for aflatoxins. *Analytica Chimica Acta*, 912, 10–23.
- Wu, Z. Q., Wang, B. C., Sun, Y. B., & Liu, Y. (2015). Improvement of determination method of Okadaic acid in shellfish by liquid chromatography-tandem mass spectrometry. *Journal of Food Safety and Quality*, 6(1), 265–271.
- Yakes, B. J., Buijs, J., Elliott, C. T., & Campbell, K. (2016). Surface plasmon resonance biosensing: Approaches for screening and characterising antibodies for food diagnostics. *Talanta*, 156, 55–63.
- Yang, S. T., Chen, S., Chang, Y. L., Cao, A. N., Liu, Y. F., & Wang, H. F. (2011). Removal of methylene blue from aqueous solution by graphene oxide. *Journal of Colloid and Interface Science*, 359(1), 24–29.
- Zendong, Z., McCarron, P., Herrenknecht, C., Sibat, M., Amzil, Z., Cole, R. B., & Hess, P. (2015). High resolution mass spectrometry for quantitative analysis and untargeted screening of algal toxins in mussels and passive samplers. *Journal of Chromatography A*, 1416, 10–21.
- Zhang, Z., Duan, H., Li, S., & Lin, Y. (2010). Assembly of magnetic nanospheres into one-dimensional nanostructured carbon hybrid materials. *Langmuir*, 26(9), 6676–6680.
- Zhang, Z., & Kong, J. (2011). Novel magnetic Fe<sub>3</sub>O<sub>4</sub>@C nanoparticles as adsorbents for removal of organic dyes from aqueous solution. *Journal of Hazardous Materials*, 193, 325–329.